Original paper

Molecular profiling of sporadic medullary thyroid carcinomas – a next-generation sequencing-based study

Serdar Altinay[1,2], Altan Kara[3], Mustafa Emre Gülbağcı[2], Ahmet Cem Dural[4], Şaban Tekin[5,6], Tuğba Kul Köprülü[6,7], Nisa Begüm Erdoğan[8], Meral Mert[9], Ülkan Çelik[10], Mustafa Turan[11,12]

[1]Department of Pathology, Hamidiye Faculty of Medicine, University of Health Sciences, Istanbul, Turkey
[2]Department of Pathology, Bakırköy Dr. Sadi Konuk Training and Research Hospital, University of Health Sciences, Istanbul, Turkey
[3]Tubitak Mam Institute of Genetic Engineering and Biotechnology, Istanbul, Turkey
[4]Departmenf of Endocrin Surgery, Medical Faculty, Istinye University, Istanbul, Turkey
[5]Department of Basic Medical Sciences, Hamidiye Faculty of Medicine, University of Health Sciences, Istanbul, Turkey
[6]Next Generation Sequencing Laboratory, Experimental Medicine Application and Research Centre, University of Health Sciences, Istanbul, Turkey
[7]Department of Medical Services and Techniques, Medical Laboratory Techniques, Hamidiye Vocational School of Health Services, University Health Sciences, Istanbul, Turkey
[8]Cerrahpaşa Medical Faculty, Istanbul University, Istanbul, Turkey
[9]Department of Endocrinology, Bakırköy Dr. Sadi Konuk Training and Research Hospital, University of Health Sciences, Istanbul, Turkey
[10]Department of Basic Medical Sciences, Department of Medical Biology, Hamidiye Faculty of Medicine, University of Health Sciences, Istanbul, Turkey
[11]Department of General Surgery, Çam and Sakura City Hospital, Istanbul, Turkey
[12]Department of Molecular Oncology, Hamidiye Institute of Health Sciences, University of Health Sciences, Istanbul, Turkey

Medullary thyroid carcinomas (MTCs) are 75% sporadic and 25% hereditary. This study aimed to determine the histopathological parameters and molecular changes of sporadic MTCs in a university hospital by targeted next-generation sequencing (NGS) including 62 genes. All *RET* mutations were missense mutations.

EIF1AX was suggested by artificial intelligence as a gene of interest for further analysis; subsequent testing revealed a pathogenic missense mutation in this gene in a patient with advanced-stage disease, who died at the 25th month of follow-up due to liver metastasis. We identified different gene mutations that could be associated with nodal metastasis in the presence or absence of *RET* mutation. We identified mutations that may be involved in tumour progression and have prognostic significance, such as *HRAS, MAP3K1*, and *EIF1AX*.

We observed *KDR* mutation in this cohort. Although driver mutations in sporadic medullary thyroid carcinoma (sMTC) mostly come from targeted NGS data in tumours from patients with localised disease, NGS findings can also be used for therapeutic purposes in advanced-stage sMTC cases with progressive local-regional or distant metastatic disease.

We believe that additional studies should be conducted with a larger number of patients so that the findings can be included in the treatment guidelines to be prepared.

Key words: thyroid, endocrine cancer, molecular, NGS, WES, mutation.

Introduction

Medullary thyroid carcinoma (MTC) accounts for 5–10% of all thyroid malignancies and occurs sporadically in 75% of cases, while the remainder develop with multiple endocrine neoplasia (MEN) 2A, MEN2B, or familial MTC (fMTC) [1–3]. Multiple endocrine neoplasia 2 syndromes, those with autosomal dominant inheritance patterns, arise as a result of germline mutations in the RET proto-oncogene (10q 11.2). Germline mutations resulting in aberrant activation of RET receptors have been characterised in MEN2A, MEN2B, and fMTC [4–6]. While RET mutations detected in sporadic MTC are in exomes 10, 11, 15, and 16, in hereditary MTC they are in exomes 5, 8, 10, 11, 12 to 16, and 19 [7]. Codon 634 mutations are found in approximately 80% of MEN2A patients, while codon 609, 618, and 620 mutations account for more than 60% of fMTC cases and patients with the Hirschsprung phenotype [3]. Central and lateral compartment lymph node metastases of patients with T4 tumours were 86% and 93%, respectively, and 70% of patients with MTC presenting with a palpable thyroid nodule had cervical metastases and 10% had distant metastases [3, 8]. Unfortunately, we have limited information about gene mutations that can predict lymph node metastasis and distant metastasis and predict disease progression.

Patients with sporadic MTC do not harbour germline RET mutations, while up to half have somatic RET mutations in their tumours [9]. The M918T mutation, seen in most patients with MEN2B, is the most common mutation in sporadic tumours and accounts for 75–95% of RET mutations and seems to predict a worse clinical course and prognosis [3, 9]. Surprisingly, RET mutations in sporadic tumours may not necessarily trigger tumourigenesis but may instead appear important for disease progression. When RET mutation is present, it shows mutational heterogeneity even in advanced disease, supported by a lower detection rate of RET mutations in sporadic microcarcinomas than in larger tumours [10].

While the M918T mutation has been reported at different rates in sporadic MTCs in different countries, in polymerase-chain reaction (PCR)-based studies conducted in our country, the M918T mutation was not detected in sporadic-type MTCs, and it was detected in only 2 patients in hereditary MTCs [11]. No M918T mutation was found in the multicentre "Turkmen" study of 56 patients [12]. In both studies, RET mutation rates were very low: 5.2% and 8.9%, respectively. However, RET mutation detected by next-generation sequencing (NGS) in the literature ranged 21–88% [9, 13–20]. Next-generation sequencing allows cost-effective screening of more samples and detection of multiple variants in targeted areas of the genome [21, 22]. Whole-exome sequencing is a widely used NGS method that involves sequencing protein-coding regions of the genome [23, 24].

Activating RAS mutations that may be associated with clinically less aggressive tumours have also been recently identified in a subset of sporadic MTCs [18]. The occurrence of RAS mutations in approximately 10–45% of RET wild-type sporadic tumours suggests that they almost always seem to be mutually exclusive with RET mutations [18, 25, 26].

Our aim is to briefly review the histopathological features of sporadic MTC with and without nodal involvement in a tertiary hospital affiliated with a university hospital, and then to investigate mutational changes by targeted NGS that will shed light on the molecular basis of nodal disease. For this purpose, we are expanding the commercially available lung-thyroid gene panel, which contains 30–36 genes, and adding genes important in molecular pathogenesis. In addition, we consider biological pathway enrichment analysis and artificial intelligence modelling for better results in a limited cohort, unlike previous studies. We think that if different mutations are detected in patients with nodal involvement, it will allow the development of new strategies for follow-up and treatment.

Material and methods

Case selection and clinicopathological features

In this retrospective study, patients diagnosed with medullary-type thyroid carcinoma in thyroidectomy material between 2007 and 2019 were included. A total of 20 cases were detected. A total of 7 cases, including 2 cases with mixed/combined medullary cancer, 2 cases with less than 30% tumour area, and 3 cases with DNA less than 10 nanograms/microlitre (ng/μl) or with insufficient DNA quality, were excluded from the study. All preparations of 13 cases included in the study were re-evaluated by a board-certified endocrine pathologist (SA). The pathological staging of the cases was performed according to the World Health Organisation (WHO) 2025 Endocrine Pathology series [27] and American Joint Committee on Cancer (AJCC) 8th edition [28]. For the study, approval was obtained from the Health Sciences University, Bakırköy Dr. Sadi Konuk Training and Research Hospital Clinical Research Ethics Committee (2019/300).

All patients in our centre underwent total thyroidectomy and central neck dissection as minimal standard procedures. If node metastases were diagnosed before surgery, lymphadenectomy of the lateral compartment(s) was performed during the initial surgical treatment.

Patients were classified as having sporadic MTC according to predefined criteria, including:

- absence of RET germline mutations confirmed by genetic testing,
- lack of a documented family history of MTC or related endocrine disorders,
- presence of other endocrine neoplasms indicative of non-hereditary disease.

Demographic data

Parameters such as age at the time of diagnosis, location, surgical procedure information, and local/distant spread in the patients can be accessed from the hospital electronic information management system. Histopathological features such as tumour diameter, encapsulation, histological tumour type, tumour grade, lymphatic-vascular-perineural invasion, surgical margin status, extra-thyroidal spread, and lymph node involvement were obtained through microscopic re-evoluation. Data on the most recent clinical status, follow-up duration, disease-free survival (DFS), and overall survival (OS) for the 13 patients who remained under observation were systematically retrieved from the endocrine surgery clinic records.

Histomorphological and immunohistochemical evaluation

Histological subtype verification was based on the WHO 2025 classification of thyroid tumours [29]. Thyroid was graded according to the new criteria defined in medullary cancers [30]. Desmoplastic stromal reaction (desmoplasia) scoring; negative (0), it was recorded as mild (1+), moderate (2+), or intense (3+) [31]. Amyloid scoring; similar to desmoplasia [32], it was recorded as negative (0), mild (1+), moderate (2+), or intense (3+). Microscopically, C-cell hyperplasia (CCH) with at least 50 cells or more in the 100× magnification field was classified as focal-nodular-diffuse as defined in the literature [33]. The pathological staging of the cases was performed according to the CAP 2023-March Thyroid Cancer Protocol [34] and AJCC 8th Edition [28]. The presence of metastases in haematoxylin and eosin sections of the lymph nodes in cases who underwent neck dissection/lymph node dissection was investigated. Previously prepared stained slides of 13 cases were used for calcitonin. Those with a calcitonin staining below 50% and those with or above 50% were grouped.

DNA isolation from samples, qualitative and quantitative analysis of DNA

DNA isolation from FFPE tissue was performed with the Quick DNA FFPE kit (Zymo Research, #D3067) in accordance with the manufacturer's protocol. 5–6 sections of 10 μm size were taken from the FFPE samples with a microtome (Leica, RM2235), transferred to 1.5 ml microcentrifuge tubes, and 400 μl of deparaffinization solution was added and incubated at 55°C for 1 minute. Then, 2X Digestion buffer and Proteinase K were added to lyse the tissues and incubated at 55°C for 12 hours. At the end of the period, the samples were incubated for a second time at 94°C for 20 minutes, and then 5 μl of RNase A was added and incubated for 5 minutes at room temperature. After adding 350 μl of Genomic Lysis Buffer, the samples were thoroughly vortexed, and then 135 μl of isopropanol was added and centrifuged at 12,000 × g for 1 minute. After centrifugation, the supernatant was added to the filtered spin column and centrifuged at 10,000 × g for 1 minute, allowing the DNA to adhere to the spin column. After 2 separate washes with Genomic DNA Wash Buffer 1 and 2, DNA from the spin column was eluted using 50 μl of DNA Elution Buffer. Qualitative and quantitative analyses of the obtained DNAs were performed on a TapeStation 4150 (Agilent) device using the Genomic DNA ScreenTape Assay kit and Qubit 4.0 fluorometer using the dsDNA BR Assay Kit, respectively. The OD260/280 values of the samples were recorded with the Synergy Neo 2 Multi-Mode reader (BioTek) using a Take 3 Plate. Samples with a DIN value of ≥ 7, an OD260/280 value of 1.8–2.0, and a concentration above 20 ng/μl were included in the study. Since the library preparation took place immediately after DNA isolation, the isolated DNA samples were stored at +4°C.

Targeted next-generation sequencing library preparation

Library preparation of DNAs obtained from formalin-fixed paraffin-embedded (FFPE) tissues was carried out in the Health Sciences University Experimental Medicine Application and Research Centre New Generation Sequencing laboratory using Sure Select XT HS/Low Input Target Enrichment with a Pre-Capture Pooling kit (Agilent). Prior to library preparation, each genomic DNA (gDNA) sample, whose concentration was determined, was diluted to 100 ng gDNA in 50 μl using 1X TE Low TE buffer. Diluted gDNA samples were fragmented using the SureSelect XT HS and XT Low Input Enzymatic Fragmentation kit, and DNA fragments of 150–200 bp were obtained. Then, non-templated nucleotide was added to the 3' end of the DNA with the Repair and dA-Tail process, and 25 μl of Ligation Master Mix and 5 μl of Adapter Oligo Mix specific for each sample were added to the samples with a volume of approximately 70 μl, and adapters were attached to the samples. Adapter bound libraries obtained after washing using AMPure XP beads were amplified by Pre-Capture PCR Amplification. Unwanted fragments in the amplified library samples were removed with AMPure XP beads, and the prepared library samples were analysed using the D1000 ScreenTape Assay kit. Equal volumes of each sample were

taken, and 8 samples were pooled in one tube – a total of 1500 ng indexed samples were hybridised using Capture Library and SureSelect Fast Hybridization Buffer. The hybridised library samples were captured with Streptavidin-coated beads and eluted from the beads, and then the obtained libraries were amplified by Post Capture PCR Amplification. The amplified library samples were washed using AMPure XP beads, and the library samples retained by the beads were dissolved with 25 μl of Low TE buffer, and the library concentration and size were measured in the TapeStation 4150 device with the High Sensitivity D1000 kit. After determining the concentration of each library, library samples were stored at –20°C until sequencing.

Analysis of targeted next-generation sequencing libraries

Prepared library samples were prepared for analysis using the NovaSeq 6000 Sequencing System Guide. The resulting library samples were pooled to 2nM and denatured with 0.2 NaOH after the addition of 2.5 nM PhiX. The analyses of denatured libraries containing PhiX were performed on a Novaseq 6000 using the SP flowcell 300 cyc kit.

Gene panel

Samples containing sufficient and high quality DNA were collected as planned with 62 genes (*ABL1, AKT1, ALK, AXL, APC, ATM, BRAF, CALCA, CCND1, CDH1, CSF1R, CTNNB1, DDR2, EGFR, ERBB2, FBXW, FGFR1, FGFR2, FGFR3, GNA11, GNAQ, GNAS, HNF1α, HRAS, IDH1, IDH2, JAK2, JAK3, KDR, KIT, KRAS, KRT20, KRT7, MAP2K1, MET, MLH1, MPL, NOTCH1, NPM1, NRAS, NRG1, NTRK1, NTRK2, NTRK3, PIK3CA, PPARG, PTEN, PTH, PTPN11, RB1, RAF1, RET, ROS1, SLC5A5, SMAD4, SMARCB1, SMO, SRC, STK11, THADA, TP53, TTF1, VHL*). The commercially available lung-thyroid gene panel, which contained 30–36 genes, was expanded to include genes important in molecular pathogenesis.

Since medullary cancers are mostly associated with the RET gene, we focused primarily on the RET gene on the 10th chromosome. At the same time, the M918T mutation in exon 16, which is the most common mutation in sporadic tumours, was investigated.

Biological pathway enrichment method and artificial intelligence modelling

A biological pathway enrichment analysis was performed based on the Kyoto Encyclopaedia of Genes and Genomes (KEGG) database to be used in the next step of the study [35]. If a pathway listed in this way was predicted to be an interesting finding for the target disease, it would be possible to examine other genes involved in the relevant pathway but not in the 62-gene list. All patients were evaluated using CHASMplus_THCA [36, 37]. In our study, this software, which was especially trained on thyroid cancer, showed mutations that could be driver or passenger for the relevant patient in the data presented to us.

Statistical method

Statistical Package for the Social Sciences (SPSS 25.0) software was used to analyse the data. Quantitative results were expressed as arithmetic mean ± standard deviation. The χ^2 test was used to examine the dependence, i.e. the relationship, between the data groups with the categorical data type. To investigate whether there is a statistical difference between the groups, the Mann-Whitney *U* test, which is one of the non-parametric tests, was used because the number of samples in the continuous data was less than 20.

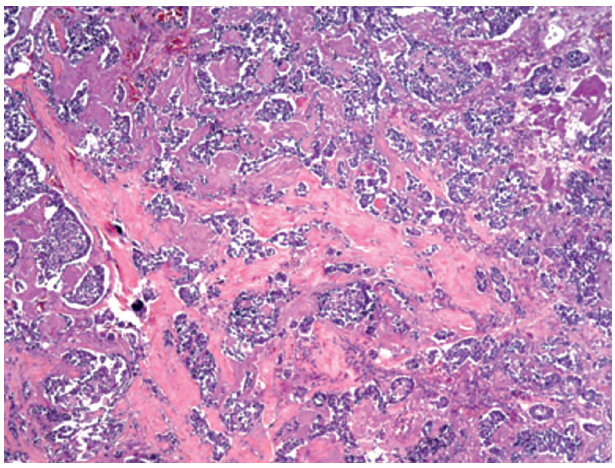

Figure 1. The picture shows a microscopic image of a patient with a RET mutation negative, EIF1AX mutation positive, nodal metastasis, and a desmoplasia score of 3+ (HE; 40×)

Results

Demographic, clinical, and pathological findings

The age range of the 13 patients included in the study was 26–68 years, with a mean of 50.4 ±14.8, and a median value of 55. The number of female patients was 10 (77%), the number of male patients was 3 (23%), and the female/male ratio was 10/3 = 3.33. While 2 (15%) of the patients included in the study had desmoplasia, 11 (85%) did not have desmoplasia. Among all patients in the study, one patient with the most severe desmoplasia, a score of 3+ (Figure 1), was unique in demonstrating capsular invasion, lymphatic invasion, and angioinvasion. She had positive surgical margins and had extrathyroidal spread. Liver metastases were detected 1 month after diagnosis, and she died of the disease at 25 months

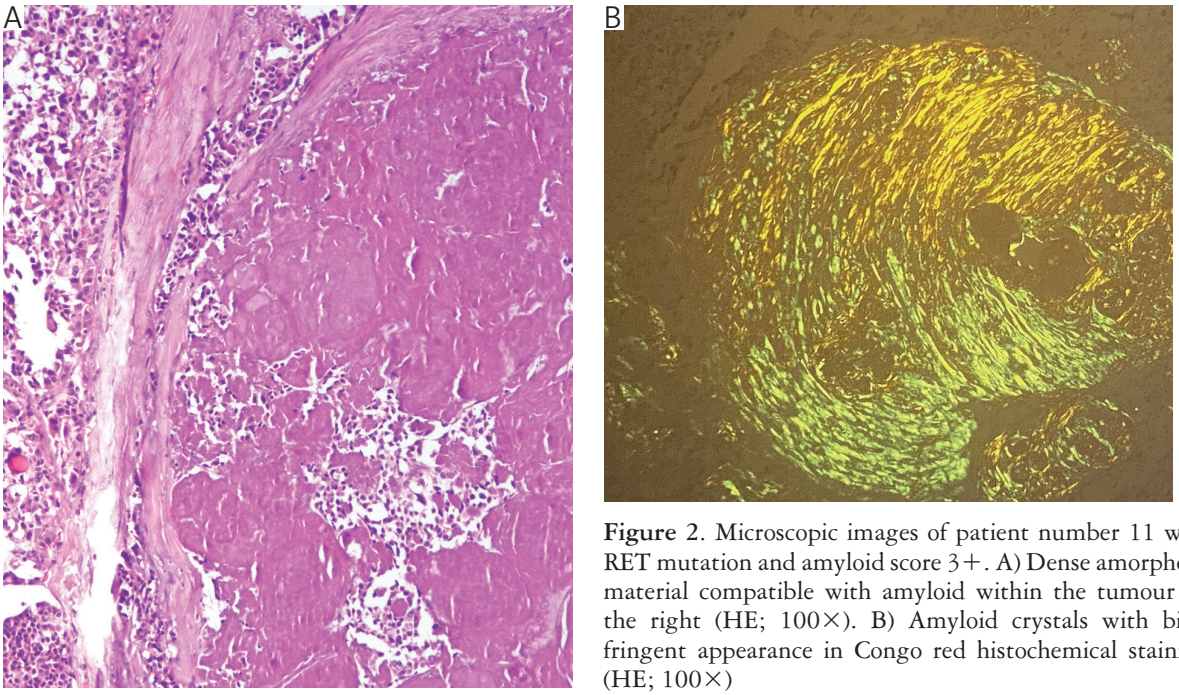

Figure 2. Microscopic images of patient number 11 with RET mutation and amyloid score 3+. A) Dense amorphous material compatible with amyloid within the tumour on the right (HE; 100×). B) Amyloid crystals with birefringent appearance in Congo red histochemical staining (HE; 100×)

of follow-up. A patient with the most intense amyloid deposition (score 3) (Figure 2) and moderate desmoplasia (score 2) on microscopic examination had 14 lymph node metastases on neck dissection: 5 on the right lateral and 9 on the left lateral. This patient was the only one with lymph node metastases among patients with RET mutations (Figure 3). Other parameters of all patients are shown in Table I. The relationship between nodal involvement and stage and capsule invasion was statistically significant ($p < 0.05$). There was no statistical relationship between all other parameters (Table II).

Considering the surgical margin status, the tumour was continuous in the surgical margin in 3 patients (23%). One of these patients (numbered 9) died due to distant metastasis. Extrathyroidal spread was present in 2 (15.3%) of the cases. While none of the tumours examined according to the new criteria showed necrosis, 2 cases had a high Ki-67 proliferation index and 5 or more mitoses (≥ 5/2 mm^2) per 2 mm^2 (patient 9; Ki-67; 10% and 8 mitosis, patient 13 [Figure 4]; Ki-67; 15% and 12 mitosis). According to the WHO 2025 classification, these 2 cases (15%) were high grade, while 11 (85%) were classified as low grade. Follow-up information was available for all patients (13/13, 100%); 1 (8%) patient died due to distant metastasis, 1 (8%) patient was alive with disease (due to high calcitonin level), and the other 11 (84%) patients were disease-free. There was no statistical relationship between other parameters.

Molecular analysis findings

While RET mutation was positive in 4 (30.8%) of the cases in the study, RET was negative in 9 (69.2%) cases. The relationship between the RET mutation and all other parameters is shown in Table III. However, no statistical relationship was found between all parameters. All RET mutations seen with the Illumina NovaSeq6000 NGS device according to the RET gene and amino acid sequences on it were missense mutations. For patients with RET mutations, changes in the amino acid sequence of the gene located on chromosome 10 were identified and mapped to the following codons: patient 1: c.1902C>G p.Cys634Trp (exon 11). Patient 7: (14730) c.2257A>C p.Cys634Trp. Patient 11: (19616) c.2370G>T p.Leu790Phe (exome 13). Patient 13: (14805) c.1901G>T p.Cys634Phe (exome 11).

In the second stage of the study, it was ascertained whether there was a mutation specific to the patient in any of the genes included in the 62-gene list specified in the method section (Figure 5); in the patient group with RET mutation (–) LN (–); missense mutation was observed in *SMAD4, ABL1, ATM, NOTCH1, PDGFRA,* and *KDR* genes, and a stop gain was observed in the *KIT* gene. In the patient group with RET mutation (–) LN (+) missense mutations were seen in *ABL1, MLH1, NOTCH1, HRAS, GNAS, and ATM* genes. In the patient group with RET mutation (+) and LN (+) missense mutation was seen in the *KDR* and *ABL1* genes. In the patient group with RET mutation (+) and LN (–) missense mutation was observed in the *SMO, ABL1, APC, MET,* and *GNAS* genes, and a stop gained mutation in the *KIT* gene (Figure 6). The mutational status of the patients is shown in Figure 7.

Biological pathway enrichment analysis

For pathogenesis that may be associated with thyroid medullary cancer pathogenesis according to

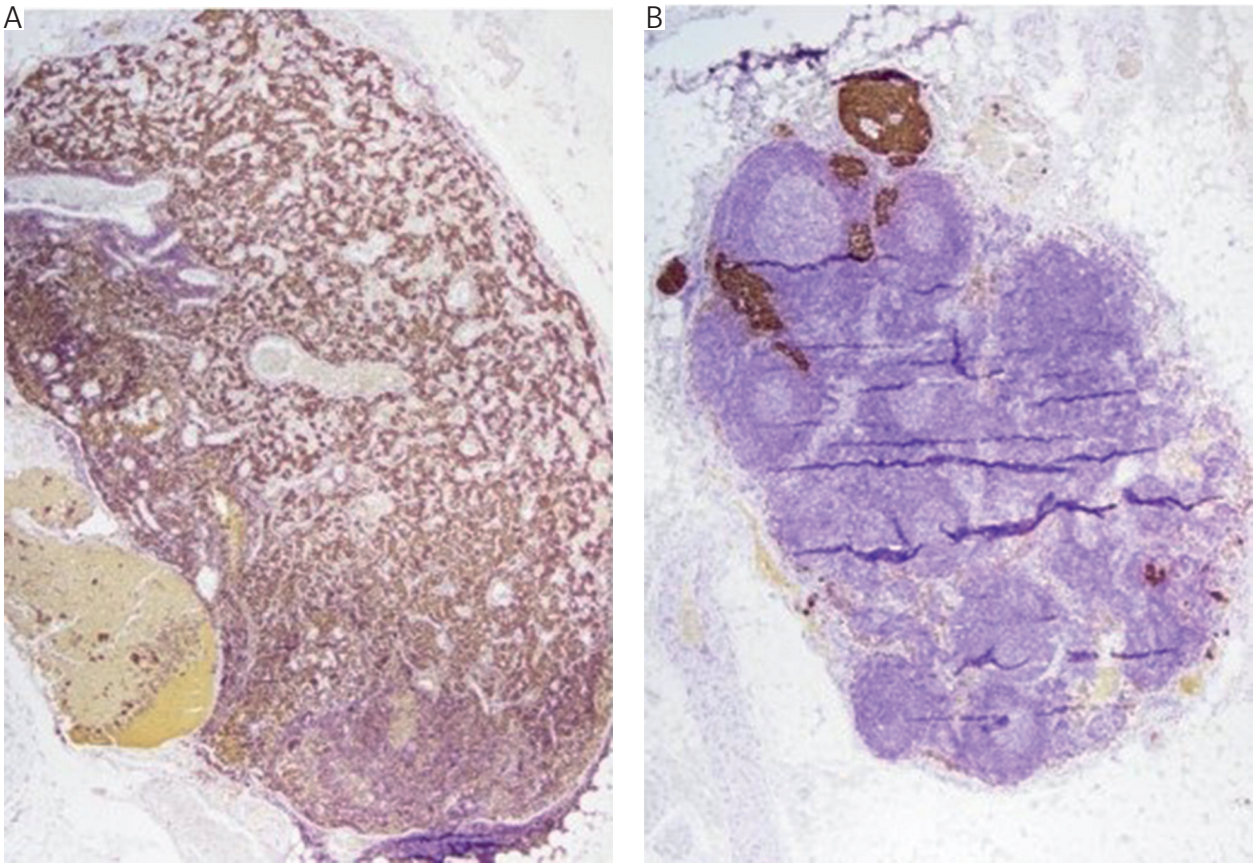

Figure 3. Images are shown of the only patient (number 11) with nodal metastasis among patients with RET mutations. Calcitonin immunohistochemistry confirming thyroid medullary cancer metastasis. On the left, the entire node is infiltrated with tumour, and on the right, the tumour is present in a few very small foci (40×)

KEGG (2021_Human_PathwayEnrichment) biological pathway enrichment analysis was reviewed. All of the genes involved in the PI3K-Akt signalling pathway, the MAPK signalling pathway, the thyroid cancer pathway, and the thyroid hormone signalling pathway were included in the 62-gene panel in the study list. *MLH1* and *HRAS* genes were noted as the determinants of lymph node metastasis in patients with (–) RET gene mutation. When cancer pathways were reviewed one by one, it was seen that *MLH1* was associated with gastric, colorectal, endometrial, mismatch repair, and Fanconi anaemia. It was noticed that *HRAS* is found in almost all pathways, and it is effective in hepatocellular carcinoma, stem cell pathway, cancer carbon metabolism pathway, and Erb signalling pathway.

Contribution of artificial intelligence modelling

In our patient group, mutations with the potential to be important on 3 genes were found with this software. While one of these genes was in our 62-gene target gene list (*HRAS*), the other 2 (*MAP3K1* and *EIF1AX*) were not present in our list. Here, especially the mutation on MAP3K1 (c.2416G>A p.Asp806Asn) was seen in many of our patients (numbered 1, 2, 3, 5, 6, 9, and 10), but it was seen as homozygous in only the 5th patient and heterozygous in the others. All mutations in the *MPA3K1* gene were pathogenic and missense (Table IV). Three of the patients with lymph node metastases (nos. 2, 5, and 9) showed this mutation.

The other gene not in our list of 62 genes is *EIF1AX*, and only one patient (number 9) had an EIF1AX mutation (c.221C>T p.Ser74Leu). This patient with pathogenic and missense mutation was advanced stage (pT3N1M1). He died in the 25th month of follow-up due to liver metastasis.

Discussion

Medullary thyroid carcinoma is a relatively uncommon tumour type, accounting for 5% or less of thyroid malignancies. However, it causes a disproportionate number of thyroid cancer deaths due to its more aggressive clinical behaviour compared to well-differentiated papillary and follicular thyroid carcinomas [1–3]. Demographic data of the patients in the study are presented in Table I. No significant correlation was found between other histopathological parameters and nodal metastasis, except for stage and capsular invasion. Medullary thyroid carcino-

Table I. Clinicopathologic characteristics of patients with sporadic medullary thyroid carcinoma

(n = 13)

Parameters	Patient numbers												
	p1	p2	p3	p4	p5	p6	p7	p8	p9	p10	p11	p12	p13
Age	39	64	36	53	26	62	68	38	60	55	66	29	60
Year of operation	2019	2016	2012	2020	2016	2018	2016	2009	2018	2017	2019	2016	2018
Tumour size [cm]	1,8	3,5	0,8	0,8	0,5	2	1,9	5	2,6	0,3	2,2	4,5	2,3
pTNM	T1bN0	T2N1	T1N0	T1N0	T1N1	T1N0	T1bN0	T3N1	T3N1M1	T1N0	T3N1	T3N1	T3N0
Distant metastasis	No	No	No	No	No	No	No	No	liver	No	No	No	No
DFS	40	32	119	35	68	56	67	89	25	65	39	65	58
OFS	40	32	119	35	68	56	67	89	25	65	39	65	58
Status	ADF	ADF	ADF	ADF	ADF	ADF	ADF	ADF	Ex	ADF	ADF	AWD	ADF
RET mutation	p.Cys634Trp	(–)	(–)	(–)	(–)	(–)	p.Cys634Trp	(–)	(–)	(–)	p.Leu790Phe	(–)	p.Cys634Phe
Desmoplasia score	0	0	0	0	0	0	0	0	3+	0	2+	0	0
Amyloid score	2+	0	0	0	0	2+	0	1+	0	1+	3+	1+	0
C-cell Hyperplasia	No	Yes	Yes	No	No	No	Yes	No	No	No	No	No	No
Calcitonin staining (%)	≥ 50	≥ 50	≥ 50	< 50	< 50	≥ 50	< 50	< 50	< 50	< 50	≥ 50	≥ 50	≥ 50
Variant	Follicular	Pseudopapillary	Follicular	Pseudopapillary	Follicular	Pseudopapillary	Follicular	Spindle	Spindle	Follicular	Follicular	Follicular	Pseudopapillary
Focality	unifocal	unifocal	unifocal	unifocal	multifocal	unifocal	unifocal	unifocal	unifocal	unifocal	multifocal	unifocal	unifocal
Surgical margin	(–)	(–)	(–)	(–)	(–)	(–)	(–)	(–)	(+)	(–)	(–)	(+)	(+)
Necrosis	No	No	No	No	No	No	No	No	No	No	No	No	No
Grade	Low	Low	Low	Low	Low	Low	Low	Low	High	Low	Low	Low	High
Capsule invasion	(–)	(–)	(–)	(+)	(–)	(–)	(–)	(+)	(+)	(–)	(–)	(–)	(+)
Encapsulation	No capsule	No capsule	No capsule	Focal	No capsule	No capsule	No capsule	Focal	Focal	No capsule	No capsule	No capsule	Encapsule
ETE	(–)	(–)	(–)	(–)	(–)	(–)	(–)	(+)	(+)	(–)	(–)	(–)	(–)
Lymphatic invasion	(–)	(–)	(+)	(–)	(–)	(–)	(–)	(+)	(+)	(–)	(+)	(+)	(–)
Angioinvasion	(–)	(–)	(–)	(–)	(–)	(–)	(–)	(–)	(+)	(–)	(–)	(–)	(–)

** Ex patient*

ADF – alive disease free, AWD – alive with disease, DFS – disease free survival, ETE – extrathyroidal spread, OFS – overall free survival

Characteristic parameters that stand out in patients are marked in bold.

Table II. Distribution of all parameters according to the lymph node metastasis

Parameters	Lymph node metastasis		*p*-value
	Negative (%)	Positive (%)	
Gender			
Male	2 (28.6)	1 (16.7)	0.6a
Female	5 (71.4)	5 (83.3)	
RET mutation			
Negative	4 (57.1)	5 (83.3)	0.3a
Positive	3 (42.9)	1 (16.7)	
Stage			
pT1	6 (85.7)	1 (16.7)	0.02a,
pT2	–	1 (16.7)	
pT3	1 (14.3)	4 (66.7)	
Status			
Ex	–	1 (16.7)	0.25a
ADF	7 (100)	4 (66.7)	
AWD	–	1 (16.7)	
Desmoplasia			
0	7 (100)	4 (66.7)	0.25a
2+	–	1 (16.7)	
3+	–	1 (16.7)	
Amyloid			
0	4 (57.1)	3 (50)	0.33a
1+	1 (14.3)	2 (33.3)	
2+	2 (28.6)	–	
3+	–	1 (16.7)	
Subtype			
Follicular	4 (57.1)	3 (50)	0.21a
Pseudopapillary	3 (42.9)	1 (16.7)	
Spindle	–	2 (33.3)	
Focality			
Unifocal	7 (100)	4 (66.7)	0.10a
Multifocal	–	2 (33.3)	
Surgical margin			
Negative	6 (85.7)	4 (66.7)	0.42a
Positive	1 (14.3)	2 (33.3)	
Calcitonin staining (%)			
< 50%	3 (42.9)	3 (50)	0.80a
≥ 50%	4 (57.1)	3 (50)	
Grade			
Low	6 (85.7)	5 (83.3)	0.91a
High	1 (14.3)	1 (16.7)	

Table II. Cont.

Parameters	Lymph node metastasis		*p*-value
	Negative (%)	Positive (%)	
C-cell hyperplasia			
No	6 (85.7)	6 (100)	0.34a
Yes	1 (14.3)	–	
Capsule invasion			
No	5 (71.4)	1 (16.7)	0.05a,
Yes	2 (28.6)	5 (83.3)	
Lymphatic invasion			
No	6 (85.7)	2 (33.3)	0.05a
Yes	1 (14.3)	4 (66.7)	
Encapsulation			
No capsule	5 (62.5)	4 (80)	0.98a
Focal encapsule	2 (25)	1 (20)	
Total encapsule	1 (12.5)	–	
Extrathyroidal extension			
No	7 (100)	4 (66.7)	0.10a
Yes	–	2 (33.3)	
Angioinvasion			
No	7 (100)	5 (83.3)	0.26a
Yes	–	1 (16.7)	
DFS (mnt, mean ± SD)	62.86 ±26.52	53 ±24.84	0.63b
OS (mnt, mean ± SD)	62.86 ±26.52	53 ±24.84	0.63b
Age (year, mean ± SD)	53.29 ±11.86	47.17 ±18.25	0.63b
Tumour size (cm, mean ± SD)	1.41 ±0.76	3.05 ±1.65	0.05b

$p < 0.05$
[a] χ^2 test statistic
[b] Mann-Whitney U test statistic
ADF – alive disease free, AWD – alive with disease

mas have a high propensity for nodal involvement, with positive lymph nodes identified in the majority of cases [8, 38]. Researchers reported nodal disease in 40–75% of patients [39, 40]. In our study, the rate of lymph node involvement was 46%.

One of the most important prognostic factors for medullary thyroid cancer is stage [41, 42]. In our study, the stage status of 85.7% of the patients without lymph node metastasis was pT1; the stage of 66.7% of those with lymph node metastases was pT3. Patients with lymph node metastases were at a higher stage ($p < 0.05$). The inverse relationship between lymph node metastasis and stage is similar in the literature [43, 44].

Encapsulation is a strong indication of the absence of lymphatic spread of the disease [45]. A recent study supports that encapsulated tumours do not show lymph node metastasis and are associated with a better prognosis [46]. In our study, 6 of the non-encapsulated or focally encapsulated tumours did not have metastases, while 5 had lymph node metastases. This situation is not statistically significant. However, capsular invasion is significantly higher in patients with lymph node metastases than in patients without lymph node metastases. In addition, focal encapsulation of the tumour of the ex-patient can be considered as a sign that non-encapsulated tumours will have a worse course.

In the long-follow-up patient series in which 289 patients were followed for 20 years (mean 8.9 years) in the literature, there is a cure that reaches 67% in pT1 stage, while this rate decreases to 50% in pT4 [47]. In our study, there was no difference between the patients followed for an average of 5.2 years in terms of stage and DFS/OS. However, the significant relationship between the incidence of a higher stage in patients with lymph node metastasis than in patients without lymph node metastasis indicates that

Table III. Distribution of all parameters according to the RET mutation

Parameters	RET Mutation		*p*-value
	Negative (%)	Positive (P)	
Gender			
Male	2 (22.2)	1 (75)	0.91a
Female	7 (77.8)	3 (25)	
Lymph node metastasis			
No	4 (44.4)	3 (75)	0.31a
Yes	5 (55.6)	1 (25)	
Staging			
pT1	5 (62.5)	2 (40)	0.81a
pT2	1 (12.5)	1 (20)	
pT3	2 (25)	2 (40)	
Status			
Ex	1 (11.1)	–	0.59a
ADF	7 (77.8)	4 (100)	
AWD	1 (11.1)	–	
Desmoplasia			
0	8 (88.9)	3 (75)	0.25a
2+	–	1 (25)	
3+	1 (11.1)	–	
Amyloid			
0	5 (55.6)	2 (50)	0.27a
1+	3 (33.3)	–	
2+	1 (11.1)	1 (25)	
3+	–	1 (25)	
Subtype			
Follicular	4 (44.4)	3 (75)	0.49a
Pseudopapillary	3 (33.3)	1 (25)	
Spindle	2 (22.2)	–	
Focality			
Unifocal	8 (88.9)	3 (75)	0.52a
Multifocal	1 (11.1)	1 (25)	
Surgical margin			
Negative	7 (77.8)	3 (75)	0.91a
Positive	2 (22.2)	1 (25)	
Calcitonin staining (%)			
< 50%	5 (55.6)	1 (25)	0.31a
≥ 50%	4 (44.4)	3 (75)	
Grade			
Low	8 (88.9)	3 (75)	0.52a
High	1 (11.1)	1 (25)	

Table III. Cont.

Parameters	RET Mutation		*p*-value
	Negative (%)	Positive (P)	
C-cell hyperplasia			
No	9 (100)	3 (75)	0.12a
Yes	–	1 (25)	
Capsule invasion			
No	4 (44.4)	2 (50)	0.85a
Yes	5 (55.6)	2 (50)	
Lymphatic invasion			
No	5 (55.6)	3 (75)	0.51a
Yes	4 (44.4)	1 (25)	
Encapsulation			
No capsule	6 (66.7)	3 (75)	0.53a
Focal encapsule	3 (33.3)	–	
Total encapsule	–	1 (25)	
Extrathyroidal extension			
No	7 (77.8)	4 (100)	0.31a
Yes	2 (22.2)	–	
Angioinvasion			
No	8 (88.9)	4 (100)	0.49a
Yes	1 (11.1)	–	
DFS (mnt, mean ± SD)	61.56 ±29.72	51 ±13.78	0.83b
OS (mnt, mean ± SD)	61.56 ±29.72	51 ±13.78	0.83b
Age (year, mean ± SD)	47 ±14.79	58.25 ±13.28	0.11b
Tumour size (cm, mean ± SD)	2.22 ±1.78	2.05 ±0.24	1.00b

$p < 0.05$
[a] χ^2 test statistic
[b] Mann-Whitney U test statistic
ADF – alive disease free, AWD – alive with disease

there may be an indirect relationship with survival when the number of patients is increased. There is no significant difference in survival between patients with RET mutation (+/–) and lymph node metastasis (+/–) (Table II, III). Undoubtedly, the small number of patients is the biggest factor in this.

Inherited forms of MTC result from autosomal dominant mutations of the RET proto-oncogene with incomplete penetration, often presenting as multifocal disease against the background of CCH. Sporadic forms may also have CCH, which requires screening of family members [48]. However, Kaserer *et al*. [49] mentioned that these criteria are not reliable for the individual patient in estimating whether there is a familial risk. Neoplastic CCH with nodular pattern was observed in only 1 patient (7.7%) among the cases. Patient 7 showed RET mutation and was

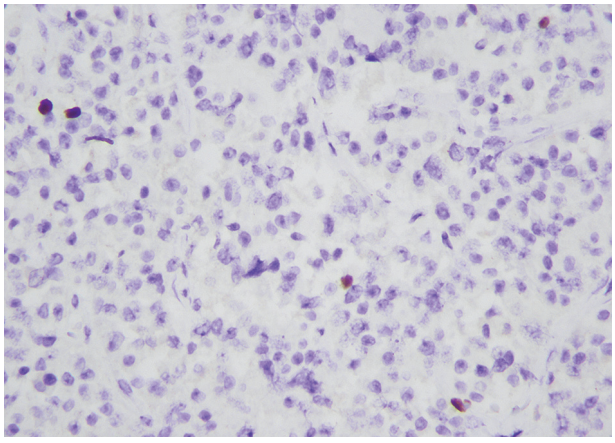

Figure 4. Microscopic image of patient number 13, which has a high grade and RET mutation
Ki-67 staining is > 5/2 mm² in the image (HE; 400×)

Variant_Annotation						PatientSpecificVariants_TargetG				1000_Genomes	CADD_Exome	
Chrom	Position	Ref_Base	Alt_Base	Gene	Transcript	Sequence_Ontology	cDNA_change	Protein_Change	Samples	AF	Score	Phred
chr7	129212026	C	T	SMO	ENST00000249373.8	missense_variant	c.1939C>T	p.Pro647Ser	Patient 1	0,002995208	3,198095	23,9
chr9	130714339	A	G	ABL1	ENST00000372348.7	missense_variant	c.20A>G	p.Lys7Arg	Patient 1		2,803029	23
chr10	43114502	C	G	RET	ENST00000355710.8	missense_variant	c.1902C>G	p.Cys634Trp	Patient 1		3,769394	25,7
chr9	136515524	C	T	NOTCH1	ENST00000651671.1	missense_variant	c.1862G>A	p.Arg621His	Patient 6	0,000599042	3,036301	23,5
chr9	136523109	-	GGAGGC	NOTCH1	ENST00000651671.1	inframe_insertion	c.439_483dup	p.Asn147_Ser161dup	Patient 6			
chr4	54727915	A	T	KIT	ENST00000288135.5	stop_gained	c.1867A>T	p.Lys623Ter	Patient 6		7,882092	40
chr5	112766328	A	T	APC	ENST00000257430.9	missense_variant	c.138A>T	p.Glu46Asp	Patient 7		3,782701	25,8
chr5	112839717	C	T	APC	ENST00000257430.9	missense_variant	c.4123C>T	p.His1375Tyr	Patient 7		3,374097	24,3
chr7	116763168	C	T	MET	ENST00000318493.11	missense_variant	c.2537C>T	p.Ser846Phe	Patient 7		3,779189	25,7
chr10	43116704	A	C	RET	ENST00000355710.8	missense_variant	c.2257A>C	p.Thr753Pro	Patient 7		3,956258	26,7
chr16	68813425	ATG	-	CDH1	ENST00000261769.10	inframe_deletion	c.1256_1258del	p.Asp419del	Patient 7			
chr4	54738462	C	T	KIT	ENST00000288135.5	stop_gained	c.2836C>T	p.Arg946Ter	Patient 13		6,7554	36
chr5	112835165	G	A	APC	ENST00000257430.9	missense_variant	c.1958G>A	p.Arg653Lys	Patient 13		6,511168	36
chr10	43114501	G	T	RET	ENST00000355710.8	missense_variant	c.1901G>T	p.Cys634Phe	Patient 13		4,321417	29,8
chr20	58853749	A	G	GNAS	ENST00000371100.8	missense_variant	c.484A>G	p.Met162Val	Patient 13	0,001996805	1,614745	16,47
chr3	37025815	G	A	MLH1	ENST00000231790.7	missense_variant	c.1217G>A	p.Ser406Asn	Patient 8	0,000399361	1,20801	13,7
chr9	136505767	G	A	NOTCH1	ENST00000651671.1	missense_variant	c.4129C>T	p.Pro1377Ser	Patient 8	0,006389776	0,058353	1,744
chr11	533874	T	A	HRAS	ENST00000311189.8	missense_variant	c.182A>T	p.Gln61Leu	Patient 8		3,884468	26,3
chr20	58854392	C	T	GNAS	ENST00000371100.8	missense_variant	c.1127C>T	p.Pro376Leu	Patient 8	0,018170927	2,126701	20,3
chr4	54273560	C	G	PDGFRA	ENST00000257290.10	missense_variant	c.1388C>G	p.Thr463Ser	Patient 10		1,226598	13,84
chr4	55106779	A	G	KDR	ENST00000263923.5	missense_variant	c.1444T>C	p.Cys482Arg	Patient 10	0,008985623	3,622067	25,1
chr9	130884406	G	A	ABL1	ENST00000318560.6	missense_variant	c.2116G>A	p.Gly706Ser	Patient 3	0,001597444	0,207275	3,207
chr11	108272729	C	G	ATM	ENST00000278616.8	missense_variant	c.3161C>G	p.Pro1054Arg	Patient 3	0,009185304	2,708381	22,8
chr18	51058396	C	T	SMAD4	ENST00000342988.8	missense_variant	c.844C>T	p.His282Tyr	Patient 3		2,16917	20,6
chr9	130885205	C	T	ABL1	ENST00000318560.6	missense_variant	c.2915C>T	p.Ser972Leu	Patient 5	0,018570288	0,255974	3,774
chr4	55102484	C	T	KDR	ENST00000263923.5	missense_variant	c.2012G>A	p.Gly671Glu	Patient 11	0,000399361	1,841894	18,04
chr9	130884325	T	G	ABL1	ENST00000318560.6	missense_variant	c.2035T>G	p.Ser679Ala	Patient 11	0,000399361	0,281598	4,074
chr10	43118458	G	T	RET	ENST00000355710.8	missense_variant	c.2370G>T	p.Leu790Phe	Patient 11	0,000199681	2,593608	22,6
chr11	108345780	T	A	ATM	ENST00000278616.8	missense_variant	c.8456T>A	p.Val2819Asp	Patient 12		0,733395	8,76
chr9	136510659	G	A	NOTCH1	ENST00000651671.1	missense_variant	c.2734C>T	p.Arg912Trp	Patient 9	0,000399361	3,710465	25,4

Figure 5. Mutations seen only in the relevant patient in the next-generation sequencing analysis

RET mutation is seen only in patients 1, 7, 11, and 13.

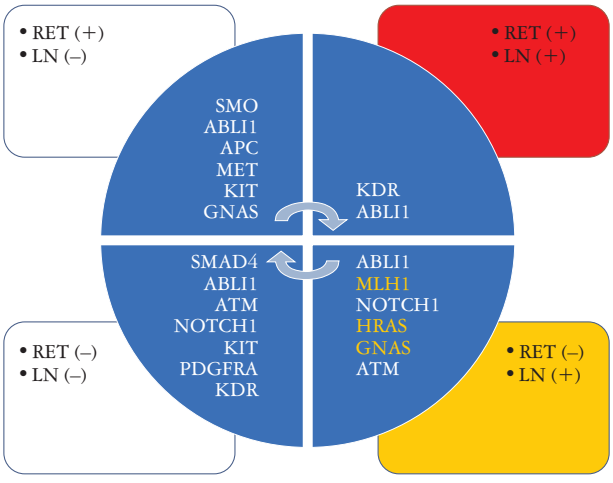

Figure 6. Gene mutations according to RET mutation and lymph node metastasis status

Note that the KDR mutation is only seen in nodal metastases from RET-positive patients. Similarly, note that MLH1, HRAS, and GNAS mutations are only seen in nodal metastases from RET-negative patients

not associated with MEN, and calcitonin elevation was not observed in the screening of family members. In the sporadic MTC series of 27 cases, 8 physiological and 3 neoplastic (11.1%) CCH were observed [48].

After the demonstration that medullary thyroid cancers with desmoplasia are associated with lymph node metastasis, the presence of this parameter in tumour histology has become important [31]. Among the cases analyzed, two exhibited desmoplasia – one moderate and one severe – both associated with lymph node metastases. A multicentre study has shown that initial lateral neck dissection is unnecessary in patients with MTC whose tumours do not exhibit desmoplastic stromal reactions; desmoplasia should be included as a morphologic parameter of exceptional clinical importance for the surgeon [49].

Given the limited number of cases in this cohort, it was necessary to focus on molecular findings, given that histological parameters were not strong enough to find out how they affect the outcome.

In this molecular oncology-based study, in addition to the lung-thyroid gene panel examined by previous investigators in sporadic MTCs [14], 16 more genes important in molecular pathogenesis were added and whole exome analysis of 62 genes was performed. The receptor tyrosine kinase (RTK) RET can be activated oncogenically by gene fusions or point mutations [50, 51]. RET fusions occur in a variety of malignancies, including 1–2% of lung cancers,

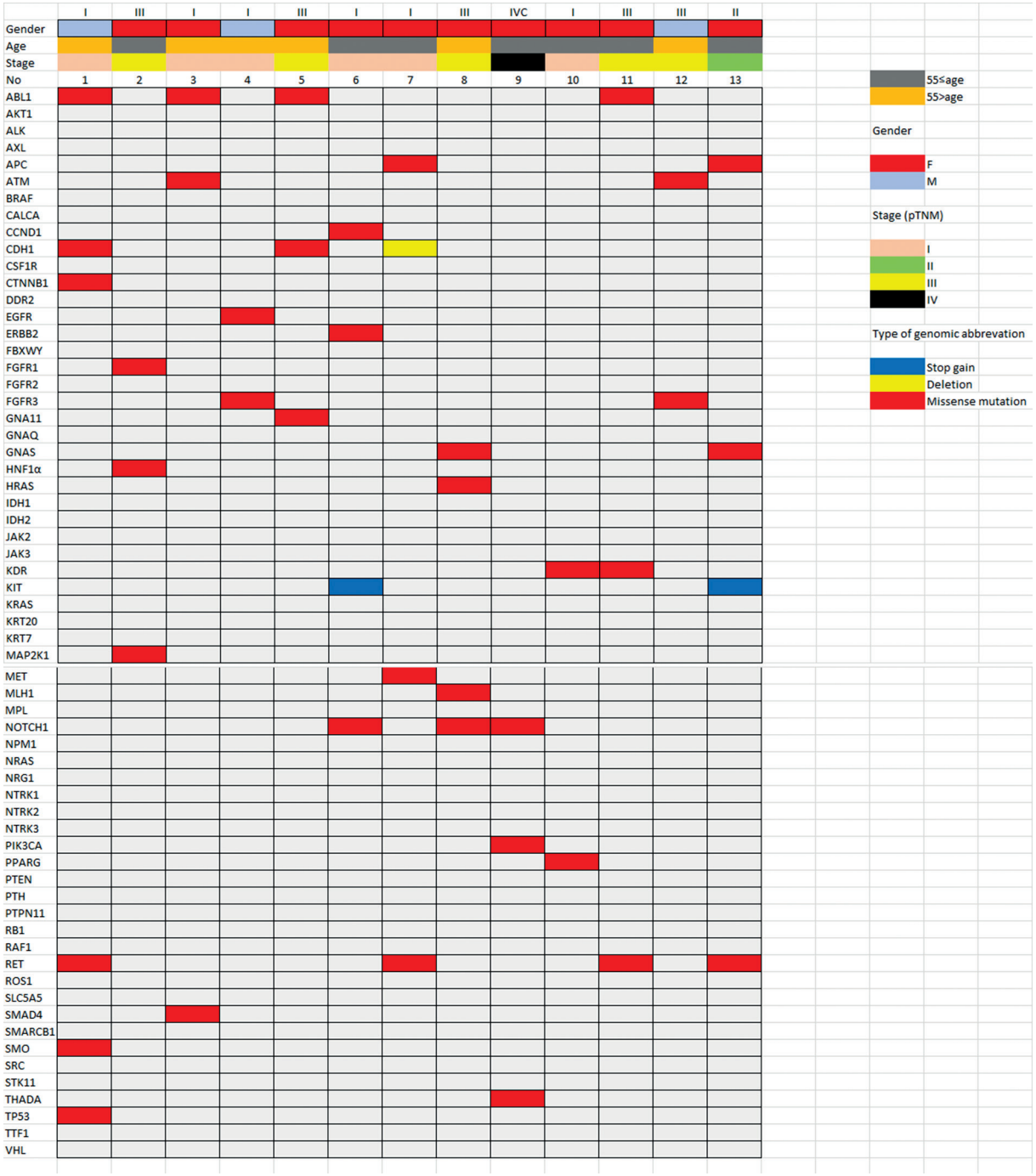

Figure 7. Genomic characterisation of sporadic medullary thyroid carcinoma by age, sex, stage, and mutation

up to 10–20% of papillary thyroid cancers, and rarely many other solid tumours [52, 53]. RET mutations affect most (about 80%) MTCs, and NGS analysis of a large number of patient tumours revealed low-frequency RET changes in other tumour types [53]. In our study, RET mutation was observed in 4 (30.8%) of 13 patients.

In the literature, RET mutation detected by NGS on blood/paraffin tissue/fresh tissue varied between 5.2 and 88% (9.13–20). Data on the number of patients, methods, and countries are shown in Table IV. All *RET* mutations seen in the current study according to the *RET* gene and amino acid sequences on it were missense mutations (c.1902C>G p.Cys634Trp, c.2257A>C p.Thr753Pro, c.2370G>T p.Leu790Phe, c.1901G>T p.Cys634Phe). Two studies on MTC in our country are PCR-based. Aydoğan *et al*. [11] in blood samples, the authors found RET mutations (Cys634arg in 3, Val804Met in 3, Cys618Ser in one, Y790Phe in one) in 8 patients (5.2%) in 154 sporadic MTCs. Compared to the study with the lowest RET mutation rate in the literature,

Table IV. RET mutation rates in sporadic medullary thyroid carcinomas in some countries

Author	Country	Patient number	Sample	Method	SomaticRET mut (%)	Gene number or exon	M918T mut (%)
Agrawal *et al*. [18]	USA	17	Tissue	NGS	70.5	21000	NA
Aydoğan *et al*. 11]	TR	154	Blood	PCR	5.2	1	0
Heilmann *et al*. [19]	USA	34*	Tissue	HC	88	315	70
Tiedje *et al*. [13]	GER	32	Tissue	NGS	66	9	25
Wei *et al*. [14]	USA	9	Tissue	NGS	88	47 (WES)	89
Nikiforova *et al*. [4]	USA	15*	Tissue+FNA	NGS	46.6	12	NA
Simbolo *et al*. [17]	IT	20	Tissue	NGS	65	50	50
Dvorakova *et al*. [9]	CZ	48	Tissue	PCR	48	10, 11, 15, 16	NA
Diwaker *et al*. [20]	West Ind.	51	Blood	PCR	21	1	NA
Qu *et al*. [57]	CN	18	Tissue	NGS	27.8	WES	20
Altinay *et al*.**	TR	13	Tissue	NGS	30.8	63 (WES)	0

** Sporadic and hereditary medullary thyroid carcinoma numbers*
*** Present study*
FNA – fine needle aspiration, HC – hybrid capture, NGS – next-generation sequence, PCR – polymerase-chain reaction, WES – whole exome sequencing

we think that the 30.8% RET mutation rate in our NGS-based study better reflects the data of our country. At the same time, we see that the amino acid changes are completely different. The multicentre EUROMEN study including hereditary MTCs showed that the most common RET mutation in the European population was Cys634, with a frequency of 67.6% [15]. The RET mutation (2/4; 50%) in patients 1 (pCys634Trp) and 13 (pCys634Phe) in our series showed that this type of mutation can be found even in such a small number of patients.

Gene analysis, which has an important place in the detection of codons, was limited to methods such as real-time PCR and microarray before 2010 [54]. Today, NGS technologies have enabled the acquisition of large amounts of data about molecules in the cell such as DNA, RNA, and micro-RNA at low cost, quickly, and in parallel [22, 54, 55]. With the advantages it brings, it has become an indispensable part of biological research carried out in many fields [21, 22, 54, 56]. For this reason, it was planned to analyse the entire exome in the 62 genes listed above, including the RET gene. Mutations were seen in exon 11 in 2 patients (50%) and in exon 13 in 2 patients (50%).

RET mutation has been reported to be a causal event in both sporadic and hereditary MTC [51]. RET mutations in exomes 10, 11, 15, and 16 are associated with sporadic MTC, while those in exomes 5, 8, 10, 11, 12, 16, and 19 are associated with hereditary MTC [7]. Most of the studies in the literature are related to familial MTCs, and the sporadic ones are either limited or the patient distribution within the series is not clear. In some of them, only the mutation rate is given, and it is not stated in which codon/exon. Considering the mutations in the series containing sporadic MTCs in Table III; Aydoğan *et al*. [11] found a 38% mutation in exon 10. Simbolo *et al*. [17], in their series of 20 cases in which they examined 50 NGS-based genes, found 65% RET mutations, including M918T (exome 16) in 10 (50%) patients, C630F in 1 (10%) patient, and C634R (exome 16) in 1 (10%) patient. Tiedje *et al.* [13] found M918T (exome 16) mutations in 8 patients (25%) in their series of 32 cases with 66% RET mutations, in which they studied 9 NGS-based genes. Wei *et al*. [14] found M918T (exome 16) mutations in 8 (89%) patients in their series of 9 cases with 88% RET mutations, in which they studied 47 NGS-based genes. Heilmann *et al*. [19] found M918T (exon 16) mutation in 21 patients (70%) in their series of 34 cases (sporadic + hereditary) with 88% RET mutation, in which they studied 315 HC-based genes. RET mutations were reported in 27.8% of 18 cases analyzed by Qu *et al*. [57] using NGS-based cancer gene panels. Specifically, C634R (exon 10) was detected in 2 patients (40%), M918T (exon 16) in 1 patient (20%), A883F (exon 15) in 1 patient (20%), and C630G (exon 11) in 1 patient (20%).

We did not find any M918T mutations in our series, of which 4 showed somatic RET mutations, and we screened all family members to be sure it was sporadic (Table IV). Aydoğan *et al*. [11] also reported that they did not detect it in sporadic MTCs but found M918T mutations in only 2 patients in hereditary MTCs. Again in our country, M918T mutation in exome 16 in a MEN2B patient was reported as a case report [58]. Erdogan *et al*. [12] did not see M918T mutation in the multicentre PCR-based Turkmen studies with 56 sporadic medullary thyroid carcinoma (sMTC) patients who appeared sporadically. Germline RET mutations were detected in a total of 6 patients (10.7%), 3 of whom were at codon

Table V. Whole exome sequencing analysis in genes found by artificial intelligence (CHASMplus*)

Variant_annotation												
Chrom	Position	Ref_ Base	Alt_ Base	Gene	Transcript	Sequence_ Ontology	cDNA_ change	Protein_Change			Samples	
chr5	56881616	G	A	MAP3K1	ENST00000399503.4	missense_ variant	c.2416G>A	p.Asp806Asn			Patient 10, patient 5, patient 3, patient 9, patient 2, patient 6, patient 1	
chr11	533874	T	A	HRAS	ENST00000311189.8	missense_ variant	c.182A>T	p.Gln61Leu			Patient 8	
chrX	20133991	G	A	EIF1AX	ENST00000379607.10	missense_ variant	c.221C>T	p.Ser74Leu			Patient 9	
		Mut.Taster			PhD-SNPg			REVEL	SIFT			VEST4
Prediction	Prediction	Functional_ Impact	Rank_ Score	Prediction	Prediction	Score	Prediction	Rank_ Score	Prediction		Zygosity	*p*-value
Damaging	Tolerated	medium	0,54805	Automatic Polymorphism	Pathogenic	0,974	Neutral	0,40416	Tolerated		het; hom; het; het; het;het;het	0,3136
Damaging	Damaging	medium	0,81001	Damaging	Pathogenic	0,996	Damaging	0,95023	Damaging		het	0,0084
	Tolerated	low	0,58761	Damaging	Pathogenic	0,984	Damaging	0,74728	Damaging		het	0,0278

**CHASMplus is a machine learning algorithm that discriminates somatic missense mutations as either cancer drivers or passengers. Predictions can be done in either a cancer type-specific manner or by a model considering multiple cancer types together (a useful default). Along with scoring each mutation, CHASMplus has a rigorous statistical model to evaluate the statistical significance of predictions. This OpenCRAVAT module represents the v1.0 precompute of CHASMplus (source code v1.0).*

634 (exome 11), one at codon 618 (exome 10), and 2 at codon 804 (exome 14). These data show that the M918T mutation, which is included in the highest risk category according to American Thyroid Association (ATA) criteria, is perhaps very rare in our country, but it needs to be proven with large series to be able to say it more decisively.

The somatic RET codon M918T mutation in sporadic MTC appears to predict an aggressive clinical course and a poor prognosis. According to the ATA risk category, medullary cancers are divided into 3 risk categories as highest (HST), high (H), and moderate (MOD) [3]. The American Thyroid Association HST category includes patients with MEN2B and RET codon M918T mutations, the ATA-H category includes patients with RET codon C634 mutations and RET codon A883F mutations, and the ATA-MOD category includes patients with RET codon mutations other than C634, A883F, and M918T. In our series, there were 2 patients (numbered 1 and 13) showing C634 mutation, who were living disease-free at 40 and 58 months of follow-up, respectively.

In a recent study [10] of 160 patients with sporadic MTC, the prevalence of somatic RET codon M918T mutations varied depending on tumour size: < 1 cm, 6 (11.3%) of 53 patients; 1–2 cm, 8 (11.8%) of 68 patients; 2–3 cm, 7 out of 22 patients (31.8%); and > 3 cm, 10 (58.8%) of 17 patients were shown to contain the M918T mutation. These data raise the question of whether RET alone acts as an initiator of oncogenesis in sporadic MTC or is subsequently activated as a driver of tumour growth along with other genes that play an important role in MTC initiation. An alternative explanation for these findings is that tumours with the M918T mutation have a high growth rate and are more likely to be diagnosed when they are larger. In our study, tumour diameters of 4 patients with RET mutation were 1.8–1.9-2.2 and 2.3. RET mutation was not observed in 2 patients who were 4 cm and above.

In this study, other gene mutations in the RET mutation-positive patients in the group with and without lymph node metastasis were compared: in the group without nodal metastases, *SMO, ABL1, APC, MET, KIT,* and *GNAS* point mutations were observed in the group with nodal metastasis; point mutations were seen in the *ABL1* and *KDR* genes. Among the RET mutation-negative patients, in the group without nodal metastases, while point mutations were observed in *SMAD4, ABL1, ATM, NOTCH1, KIT, PDGFRA,* and *KDR* genes, point mutations were detected in *ABL1, MLH1, NOTCH1, HRAS, GNAS,* and *ATM* genes in the group with nodal metastasis. Although the number of patients was low, these findings suggest that KDR mutations may be associated with nodal involvement in RET mutation-positive patients. Rodríguez-Antona *et al*. [59] reported a higher expres-

sion of KDR protein in metastatic tissues compared to primary tumour tissue of MTC patients. Tiedje *et al*. [13] also showed that a higher KDR mRNA count in MTC reflects a more aggressive tumour biology, while higher vascular endothelial growth factor receptor (VEGF) and FLT1 expression were consistent with disease-free status at follow-up. KDR, also known as VEGFR-2, (a type IV receptor tyrosine kinase) is a VEGF receptor [50]. Vandetanib ((ZD6474), a multikinase inhibitor with high affinity for VEGFR-2, is approved for the treatment of aggressive and symptomatic unresectable, locally advanced or metastatic MTC after the results of the phase III ZETA study [3]. The oncology team gave vandetanib treatment to 6 patients with lymph node metastases who had undergone total thyroidectomies. No tumour progression was observed in these patients. A remarkable point is that only one of the patients who received vandetanib (patient 11) had a *KDR* point mutation, and this patient was also positive for the *RET* mutation, among the patients with nodal involvement. Was the drug really effective in this patient, because angiogenesis was found to be highest in medullary cancers with *RET* mutants [60]?

This information indicates that VEGF receptor kinase inhibitor agents can be used in the presence of high *KDR* expression. However, if there is a RET918 mutation, it should be known that the desired response to the treatment may not be obtained. Tiedje *et al*. [13] stated that among 32 sMTC, 5 of the patients treated with vandetanib, 5 of whom had the RET918 mutation, showed partial response.

In our study, among RET mutation-negative patients, *MLH1, HRAS*, and *GNAS* mutations were observed only in those with nodal involvement, suggesting that these mutations may be associated with lymph node metastasis. Although there is no data on *GNAS* and *MLH1* mutations in the literature, the authors stated that in the absence of *RET* mutation, 56% (25), 50% (26) *H-RAS*, 12% (25), and 31% (26) *KRAS* mutations can be seen. The fact that the *RAS* mutation rate is so high suggests that alternative genes may be effective in the tumourigenesis of sporadic medullary cancer. In our study, we detected a *KRAS* mutation in only one patient (1/9; 11%).

As an added advantage of the study, other genes that may act as a driving force in tumour progression were investigated by biological pathway enrichment analysis. The pathways that may be associated with the pathogenesis of thyroid medullary cancer were reviewed. All the genes involved in the PI3K-Akt signalling pathway, MAPK signalling pathway, thyroid cancer pathway, and thyroid hormone signalling pathway were included in the 62-gene panel in the study list. Qu *et al*. [57] examined the cell cycle, *HIPPO, MYC, Notch, NRF2, PI3K, TGF*-β, RTK-*RAS, TP53,* and Wnt genes in their study by biological pathway enrichment analysis and found that 44.4% of the patients ($n = 8$) showed changes in the genes (*FAT1, FAT4, LATS2, etc*.) of the hippo pathway (cell proliferation and apoptosis).

Another difference of the current study from previous studies is the use of artificial intelligence modelling. Recent technological developments have led to the increasing application of artificial intelligence (AI) in different disciplines, one of which is oncology [61]. CHASMplus applied to 8657 samples from 32 cancer types is a modelling that identifies more than 4000 unique driver mutations in 240 genes and is also distinguished by specific cancer types [36, 61]. In our study, this software, which was especially trained on thyroid cancer, showed mutations that could be drivers or passengers for the relevant patient in the data presented to us, and as a result, mutations with the potential to be important on *HRAS, MAP3K1*, and *EIF1AX* genes were found (Table V). Of these genes, *HRAS* was in the target gene list of 62 genes, while *MAP3K1* and *EIF1AX* were not in the list.

Although the mutation in the *MAP3K1* gene (c.2416G>A p.Asp806Asn) (1,2,3,5,6,9, and 10) was seen in 7 patients (7/13; 53.8%), only the 5th patient was homozygous; the others were heterozygous. All mutations in the *MPA3K1* gene were pathogenic and missense. Three of the patients with lymph node metastases (nos. 2, 5, and 9) showed this mutation. Activation of intracellular tyrosine kinase pathways has been associated with RET mutational status. Maliszewska *et al*. [62] reported up-regulation of genes involved in Wnt, Notch, NFκB, JAK/STAT, and MAPK signalling pathways in sporadic MTC harbouring the Met918Thr RET mutation. Since the MAPK pathway is activated by the RET RTK in medullary thyroid carcinoma, the expression of BRAF and downstream mitogen-activating kinases (MAP2K1, MAP2K2, MAPK1, MAPK3) was investigated by the authors. Interestingly, the mRNA count of BRAF was found to be significantly higher in the MTC of patients who recovered disease-free after surgery compared with tumours from patients with metastatic disease [13]. In contrast, the mRNA numbers of mitogen activating kinases were similar in both subgroups.

The mechanism of MAPK activation differs in follicular cell-derived tumours from medullary thyroid cancer. While BRAF mutations frequently cause tumours of follicular cell origin, in medullary thyroid cancer, MAPK activation is mediated by RET mutations [4–6]. However, only one of our cases with MAP3K1 mutation had a RET mutation. This showed us that there may be RET mutations through some genes of non-RET origin. The fact that 3 of 7 patients with lymph node metastasis in our study had a MAP3K1 mutation was important in terms

of showing that this mutation could be associated with lymph node metastasis.

The other gene not included in our list of 62 genes is *EIF1AX*, and *EIF1AX* mutation (c.221C>T p.Ser74Leu) was seen in only one patient (#9). This patient with pathogenic and missense mutation was at an advanced stage (pT3N1M1). She died in the 25th month of follow-up due to liver metastasis. There are different reports in the literature that the EIF1AX mutation is never seen in MTCs [63] but is seen in both benign and malignant tumours [64]. Another study points out that other mutations (EIF1AX + RAS + TERT + TP53) may also be present in tumours with EIF1AX mutations [65]. We did not see RAS, TERT, and P53 mutations in patient 9 in the series. EIF1AX mutations, a component of the translation initiation complex, occur together with RAS in advanced thyroid cancers and promote tumourigenesis [66]. EIF1AX A113 splice drives an ATF4-induced dephosphorylation of EIF2a, resulting in increased protein synthesis. ATF4 also cooperates with c-MYC to sensitise mTOR to amino acids, thereby creating vulnerability to mTOR kinase inhibitors [66, 67]. The question comes to mind: if the EIF1AX mutation was known in the patient with ex, could he benefit from mTOR inhibitors? And could artificial intelligence find this vulnerability and contribute to survival?

The weakness of the study is its retrospective design and limited number of patients. One of the limiting factors is that a small amount of DNA was obtained from some patients due to preanalytical errors of paraffin blocks over 10 years. Although the follow-up information of all patients has been obtained, the presence of a few patients who discontinued treatment/follow-up negatively affects the survival analysis. However, examining the entire exome of 62 genes, including those added to the thyroid lung gene panel, performing biological pathway enrichment analysis, and applying artificial intelligence modelling for the first time in sporadic MTCs, in which different and significant mutations are found, are the strengths and uniqueness of the research.

Despite initially recruiting more patients, preanalytical errors resulted in insufficient DNA quality, leading to a reduction in sample size. This limited number of patients with and without lymph node metastasis constitutes a major limitation of the study.

Conclusions

In this first study examining sporadic thyroid medullary cancers in our country with a targeted NGS panel, we identified different gene mutations that may be associated with lymph node metastasis in the presence or absence of RET mutation. In addition, we identified mutations that may be involved in tumour progression and have prognostic significance, such as HRAS, MAP3K1, and EIF1AX, which are not included in the thyroid-lung gene panel. We showed that the KDR mutation may be important in the use of antiangiogenic drugs such as vandetanib. In light of these data, we think that it would be beneficial to expand gene panels and to question the KDR mutation when anti-VEGF-2 RTK blockers are used. Although driver mutations in sMTC mostly come from targeted NGS data in tumours from patients with localised disease, NGS findings can also be used for therapeutic purposes in advanced-stage sMTC cases with progressive local-regional or distant metastatic disease. We believe that additional studies should be conducted with a larger number of patients so that the findings can be included in the treatment guidelines to be prepared.

Disclosures

1. Institutional review board statement: The project was supported by the Scientific Research Project Coordinatorship of the University of Health Sciences (2020/105).
2. Assistance with the article: We would like to thank all the physicians of the endocrinology, oncology, and biochemistry clinics of our hospital, who evaluated our patients with great care.
3. Financial support and sponsorship: None.
4. Conflicts of interest: None.

References

1. Lloyd RV, Douglas BR, Young WF. Endocrine diseases. American Registry of Pathology and the Armed Forces Institute of Pathology, Washington 2002.
2. Livolsi VA. Surgical pathology of the thyroid. Saunders, Philadelphia 1990.
3. Wells SA, Asa SL, Dralle H, Elisei R, Evans DB, Gagel RF, et al. Revised American Thyroid Association guidelines for the management of medullary thyroid carcinoma. Thyroid 2015; 25: 567-610.
4. Nikiforov YE, Nikiforova MN. Molecular genetics and diagnosis of thyroid cancer. Nat Rev Endocrinol 2011; 7: 569-580.
5. Chernock RD, Hagemann IS. Molecular pathology of hereditary and sporadic medullary thyroid carcinomas. Am J Clin Pathol 2015; 143: 768-777.
6. Barletta JA, Nosé V, Sadow PM. Genomics and epigenomics of medullary thyroid carcinoma: from sporadic disease to familial manifestations. Endocr Pathol 2021; 32: 35-43.
7. Margraf RL, Crockett DK, Krautscheid PMF, Seamons R, Calderon FRO, Wittwer CT, et al. Multiple endocrine neoplasia type 2 RET protooncogene database: repository of MEN2-associated RET sequence variation and reference for genotype/phenotype correlations. Hum Mutat 2009; 30: 548-556.
8. Jin LX, Moley JF. Surgery for lymph node metastases of medullary thyroid carcinoma: a review. Cancer 2016; 122: 358-366.
9. Dvorakova S, Vaclavikova E, Sykorova V, Vcelak J, Novak Z, Duskova J, et al. Somatic mutations in the RET proto-oncogene in sporadic medullary thyroid carcinomas. Mol Cell Endocrinol 2008; 284: 21-27.

10. Romei C, Ugolini C, Cosci B, Torregrossa L, Vivaldi A, Ciampi R, et al. Low prevalence of the somatic M918T RET mutation in micro-medullary thyroid cancer. Thyroid 2012; 22: 476-481.
11. Aydoğan Bİ, Yüksel B, Tuna MM, Navdar Başaran M, Akkurt Kocaeli A, Ertörer ME, et al. Distribution of RET mutations and evaluation of treatment approaches in hereditary medullary thyroid carcinoma in Turkey. J Clin Res Pediatr Endocrinol 2016; 8: 13-20.
12. Erdogan MF, Gürsoy A, Ozgen G, Cakir M, Bayram F, Ersoy R, et al. Ret proto-oncogene mutations in apparently sporadic Turkish medullary thyroid carcinoma patients: Turkmen study. J Endocrinol Invest 2005; 28: 806-809.
13. Tiedje V, Ting S, Walter RF, Herold T, Worm K, Badziong J, et al. Prognostic markers and response to vandetanib therapy in sporadic medullary thyroid cancer patients. Eur J Endocrinol 2016; 175: 173-180.
14. Wei S, LiVolsi VA, Montone KT, Morrissette JJD, Baloch ZW. Detection of molecular alterations in medullary thyroid carcinoma using next-generation sequencing: an ınstitutional experience. Endocr Pathol 2016; 27: 359- 362.
15. Machens A, Niccoli-Sire P, Hoegel J, Frank-Raue K, van Vroonhoven TJ, Roeher HD, et al. Early malignant progression of hereditary medullary thyroid cancer. N Engl J Med 2003; 349: 1517-1525.
16. Nikiforova MN, Wald AI, Roy S, Durso MB, Nikiforov YE. Targeted next-generation sequencing panel (ThyroSeq) for detection of mutations in thyroid cancer. J Clin Endocrinol Metab 2013; 98: E1852-1860.
17. Simbolo M, Mian C, Barollo S, Fassan M, Mafficini A, Neves D, et al. High-throughput mutation profiling improves diagnostic stratification of sporadic medullary thyroid carcinomas. Virchows Arch 2014; 465: 73-78.
18. Agrawal N, Jiao Y, Sausen M, Leary R, Bettegowda C, Roberts NJ, et al. Exomic sequencing of medullary thyroid cancer reveals dominant and mutually exclusive oncogenic mutations in RET and RAS. J Clin Endocrinol Metab 2013; 98: E364-369.
19. Heilmann AM, Subbiah V, Wang K, Sun JX, Elvin JA, Chmielecki J, et al. Comprehensive genomic profiling of clinically advanced medullary thyroid carcinoma. Oncology 2016; 90: 339-346.
20. Diwaker C, Sarathi V, Jaiswal SK, Shah R, Deshmukh A, Thomas AE, et al. Hereditary medullary thyroid carcinoma syndromes: experience from western India. Fam Cancer 2021; 20: 241-251.
21. Shendure J, Ji H. Next-generation DNA sequencing. Nat Biotechnol 2008; 26: 1135-1145.
22. Schuster SC. Next-generation sequencing transforms today's biology. Nat Methods 2008; 5: 16-18.
23. Yang A, Zhang W, Wang J, Yang K, Han Y, Zhang L. Review on the application of machine learning algorithms in the sequence data mining of DNA. Front Bioeng Biotechnol 2020; 8: 1032.
24. Giani AM, Gallo GR, Gianfranceschi L, Formenti G. Long walk to genomics: history and current approaches to genome sequencing and assembly. Comput Struct Biotechnol J 2020; 18: 9-19.
25. Moura MM, Cavaco BM, Pinto AE, Leite V. High prevalence of RAS mutations in RET-negative sporadic medullary thyroid carcinomas. J Clin Endocrinol Metab 2011; 96: E863-868.
26. Boichard A, Croux L, Al Ghuzlan A, Broutin S, Dupuy C, Leboulleux S, et al. Somatic RAS mutations occur in a large proportion of sporadic RET-negative medullary thyroid carcinomas and extend to a previously unidentified exon. J Clin Endocrinol Metab 2012; 97: E2031-2035.
27. Endocrine and Neuroendocrine Tumors, WHO Classification of Tumors, 5th Edition, Volume 10, Lyon (France). WHO Classification of Tumours Editorial Board 2025.
28. Amin MB, Greene FL, Edge SB, Compton CC, Gershenwald JE, Brookland RK, et al. The eighth edition AJCC cancer staging manual: continuing to build a bridge from a population-based to a more "personalized" approach to cancer staging. CA Cancer J Clin 2017; 67: 93-99.
29. Organisation mondiale de la santé, Centre international de recherche sur le cancer, eds. WHO classification of tumours of endocrine organs. 4th ed. International Agency for Research on Cancer, Lyon 2017.
30. Xu B, Fuchs TL, Ahmadi S, Alghamdi M, Alzumaili B, Bani MA, et al. International medullary thyroid carcinoma grading system: a validated grading system for medullary thyroid carcinoma. J Clin Oncol 2022; 40: 96-104.
31. Koperek O, Scheuba C, Puri C, Birner P, Haslinger C, Rettig W, et al. Molecular characterization of the desmoplastic tumor stroma in medullary thyroid carcinoma. Int J Oncol 2007; 31: 59-67.
32. Albores-Saavedra J, Rose GG, Ibanez ML, Russell WO, Grey CE, Dmochowski L. The amyloıd ın solıd carcınoma of the thyroıd gland. Staınıng characterıstıcs, tıssue culture, and electron mıcroscopıc observatıons. Lab Invest 1964; 13: 77-93.
33. Perry A, Molberg K, Albores-Saavedra J. Physiologic versus neoplastic C-cell hyperplasia of the thyroid: separation of distinct histologic and biologic entities. Cancer 1996; 77: 750-756.
34. Available from: https://documents.cap.org/protocols/Thyroid_4.4.0.0.REL_CAPCP.pdf.
35. Available from: https://www.genome.jp/kegg/pathway.html.
36. Available from: https://karchinlab.github.io/CHASMplus.
37. Tokheim C, Karchin R. CHASMplus reveals the scope of somatic missense mutations driving human cancers. Cell Syst 2019; 9: 9-23.e8.
38. Polistena A, Sanguinetti A, Lucchini R, Galasse S, Monacelli M, Avenia S, et al. Timing and extension of lymphadenectomy in medullary thyroid carcinoma: a case series from a single institution. Int J Surg 2017; 41: S70-S74.
39. Saad MF, Ordonez NG, Rashid RK, Guido JJ, Hill CS, Hickey RC, et al. Medullary carcinoma of the thyroid. A study of the clinical features and prognostic factors in 161 patients. Medicine (Baltimore) 1984; 63: 319-342.
40. Gharib H, McConahey WM, Tiegs RD, Bergstralh EJ, Goellner JR, Grant CS, et al. Medullary thyroid carcinoma: clinicopathologic features and long-term follow-up of 65 patients treated during 1946 through 1970. Mayo Clin Proc 1992; 67: 934-940.
41. Schröder S, Böcker W, Baisch H, Bürk CG, Arps H, Meiners I, et al. Prognostic factors in medullary thyroid carcinomas. Survival in relation to age, sex, stage, histology, immunocytochemistry, and DNA content. Cancer 1988; 61: 806-816.
42. Al-Qurayshi Z, Khadra H, Chang K, Pagedar N, Randolph GW, Kandil E. Risk and survival of patients with medullary thyroid cancer: national perspective. Oral Oncol 2018; 83: 59-63.
43. Moses LE, Oliver JR, Rotsides JM, Shao Q, Patel KN, Morris LGT, et al. Nodal disease burden and outcome of medullary thyroid carcinoma. Head Neck 2021; 43: 577-584.
44. Hyer SL, Vini L, A'Hern R, Harmer C. Medullary thyroid cancer: multivariate analysis of prognostic factors influencing survival. Eur J Surg Oncol 2000; 26: 686-690.
45. Miccoli P, Minuto MN, Ugolini C, Molinaro E, Basolo F, Berti P, et al. Clinically unpredictable prognostic factors in the outcome of medullary thyroid cancer. Endocr Relat Cancer 2007; 14: 1099-1105.
46. Contarino A, Dolci A, Maggioni M, Porta FM, Lopez G, Verga U, et al. Is encapsulated medullary thyroid carcinoma associated with a better prognosis? A case series and a review of the literature. Front Endocrinol (Lausanne) 2022; 13: 866572.
47. Cupisti K, Wolf A, Raffel A, Schott M, Miersch D, Yang Q, et al. Long-term clinical and biochemical follow-up in medullary thyroid carcinoma: a single institution's experience over 20 years. Ann Surg 2007; 246: 815-821.

48. Guyétant S, Josselin N, Savagner F, Rohmer V, Michalak S, Saint-André JP. C-cell hyperplasia and medullary thyroid carcinoma: clinicopathological and genetic correlations in 66 consecutive patients. Mod Pathol 2003; 16: 756-763.
49. Kaserer K, Scheuba C, Neuhold N, Weinhäusel A, Haas OA, Vierhapper H, et al. Sporadic versus familial medullary thyroid microcarcinoma: a histopathologic study of 50 consecutive patients. Am J Surg Pathol 2001; 25: 1245-1251.
50. Salvatore D, Santoro M, Schlumberger M. The importance of the RET gene in thyroid cancer and therapeutic implications. Nat Rev Endocrinol 2021; 17: 296-306.
51. De Groot JWB, Links TP, Plukker JTM, Lips CJM, Hofstra RMW. RET as a diagnostic and therapeutic target in sporadic and hereditary endocrine tumors. Endocr Rev 2006; 27: 535-560.
52. Stransky N, Cerami E, Schalm S, Kim JL, Lengauer C. The landscape of kinase fusions in cancer. Nat Commun 2014; 5: 4846.
53. Kato S, Subbiah V, Marchlik E, Elkin SK, Carter JL, Kurzrock R. RET aberrations in diverse cancers: next-generation sequencing of 4,871 patients. Clin Cancer Res 2017; 23: 1988-1997.
54. Hutchison CA. DNA sequencing: bench to bedside and beyond. Nucleic Acids Res 2007; 35: 6227-6237.
55. Erdogdu IH., Orenay-Boyacioglu S, Boyacioglu O, Kahraman-Cetin N, Guler H, Turan M, et al. Microsatellite instability and somatic gene variant profile in solid organ tumors. Arch Med Sci 2024; 20: 1672-1679
56. Adamska M, Kowal-Wiśniewska E, Czerwińska-Rybak J, Kiwerska K, Barańska M, Gronowska W, et al. Defining the mutational profile of lower-risk myelodysplastic neoplasm patients with respect to disease progression using next-generation sequencing and pyrosequencing. Contemp Oncol 2023; 27: 269-279.
57. Qu N, Shi X, Zhao JJ, Guan H, Zhang TT, Wen SS, et al. Genomic and transcriptomic characterization of sporadic medullary thyroid carcinoma. Thyroid 2020; 30: 1025-1036.
58. Altaykan A, Ersoy-Evans S, Emre S, Orhan D, Güçer S, Erkin G. Multiple endocrine neoplasia type 2b associated with lichen nitidus. Eur J Dermatol 2007; 17: 292-294.
59. Rodríguez-Antona C, Pallares J, Montero-Conde C, Inglada-Pérez L, Castelblanco E, Landa I, et al. Overexpression and activation of EGFR and VEGFR2 in medullary thyroid carcinomas is related to metastasis. Endocr Relat Cancer 2010; 17: 7-16.
60. Verrienti A, Tallini G, Colato C, Boichard A, Checquolo S, Pecce V, et al. RET mutation and increased angiogenesis in medullary thyroid carcinomas. Endocr Relat Cancer 2016; 23: 665-676.
61. Kann BH, Hosny A, Aerts HJWL. Artificial intelligence for clinical oncology. Cancer Cell 2021; 39: 916-927.
62. Maliszewska A, Leandro-Garcia LJ, Castelblanco E, Macià A, de Cubas A, Goméz-López G, et al. Differential gene expression of medullary thyroid carcinoma reveals specific markers associated with genetic conditions. Am J Pathol 2013; 182: 350-362.
63. Karunamurthy A, Panebianco F, J Hsiao S, Vorhauer J, Nikiforova MN, Chiosea S, et al. Prevalence and phenotypic correlations of EIF1AX mutations in thyroid nodules. Endocr Relat Cancer 2016; 23: 295-301.
64. Simões-Pereira J, Moura MM, Marques IJ, Rito M, Cabrera RA, Leite V, et al. The role of EIF1AX in thyroid cancer tumourigenesis and progression. J Endocrinol Invest 2019; 42: 313-318.
65. Karslioglu French E, Nikitski AV, Yip L, Nikiforova MN, Nikiforov YE, Carty SE. Clinicopathological features and outcomes of thyroid nodules with EIF1AX mutations. Endocr Relat Cancer 2022; 29: 467-473.
66. Hinnebusch AG. Molecular mechanism of scanning and start codon selection in eukaryotes. Microbiol Mol Biol Rev 2011; 75: 434-467.
67. Wang Q, Holst J. L-type amino acid transport and cancer: targeting the mTORC1 pathway to inhibit neoplasia. Am J Cancer Res 2015; 5: 1281-1294.

Address for correspondence

Prof. **Serdar Altinay,** MD, PhD
Department of Pathology
Hamidiye Faculty of Medicine
University of Health Sciences,
Istanbul, Turkey
mdserdara@gmail.com